Available online at www.sciencedirect.com
SCIENCE DIRECT
Thermochimica Acta 442 (2006) 18–24
thermochimica acta
www.elsevier.com/locate/tca

Thermal properties of poly(ethylene oxide)/lauric acid blends: A SSA–DSC study

Krzysztof Pielichowski *, Kinga Flejtuch

Department of Chemistry and Technology of Polymers, Cracow University of Technology, ul. Warszawska 24, 31-155 Kraków, Poland

Available online 15 December 2005

Abstract

A series of poly(ethylene oxide) (PEO)/lauric acid blends with different compositions has been prepared and characterised by differential scanning calorimetry (DSC) in dynamic mode. It has been found that the enthalpy of melting and crystallisation reaches its highest value for PEO/lauric acid blend (1:1, w/w) which makes this system a promising candidate for thermal energy storage applications. Further studies by step-scan alternating (SSA)–DSC revealed that an increase of the temperature step causes that the average total heating rate is also increasing and the heat flow is characterised by higher values. Reversing component of the heat flow during melting reaches lowest values at highest step (step = 1°) when the re-crystallisation of PEO is hindered. An increase of step generally leads to an increase of the number of non-equilibrium effects and facilitates the activation of kinetic non-reversing processes, hindering the overall crystallisation of PEO. For lauric acid, due to facile crystallisation and self-association, formation of ordered regular structures takes place faster and is influenced by non-reversing processes in higher proportion.

Keywords: Poly(ethylene oxide); Lauric acid; Crystallisation; DSC

1. Introduction

Polymeric materials for the thermal energy storage applications are the subject of extensive research, both fundamental and applied [1–3]. Thermal energy transfer occurs during the fusion–solidification process ("Phase Change Materials"); when a PCM reaches the temperature at which it changes phase (melting point) it absorbs heat without getting hotter. When the ambient temperature in the space around the PCM material drops, the PCM solidifies, releasing its stored latent heat. PCM absorb and emit heat while maintaining a nearly constant temperature. The early studies on the energy storage issue concentrated on inorganic substances, e.g., salt hydrates, but due to non-congruent melting and corrosion the practical applicability was rather limited [4]. Recently, organic materials have been investigated as PCM and special attention has been focused on poly(ethylene oxide) which offers good physical and chemical stability, reproducible thermal behaviour without encapsulation problems and an adjustable transition zone [5,6]. Its phase behaviour should be considered in terms of both the conformation of individual molecules in the crystalline state and the arrangement of those molecules into micro- and macroscopic structures. In the crystalline state, PEO chain (which has dihedral symmetry, two-fold axes, one passing through the oxygen atoms and the other bisecting the carbon–carbon bond) contains seven structural units and two helical turns per fibre identity period of 19.3 Å—on melting, this helical structure is lost and a liquid containing random coils is obtained [7]. In the crystal lattice, PEO is arranged in form of lamellae and the chains are either in an extended or folded forms [8].

Simultaneously, fatty acids have a relatively high latent heating and exhibit small volume changes during the phase transition [9]. Since the key issue related to PCM is their phase transition behaviour we focused on the investigations of this particular phenomenon by applying the advantageous option of the differential scanning calorimetry (DSC)–step-scan alternating (SSA)–DSC which makes it possible to separate the total heat flow into the reversing and non-reversing components; the additional features of MDSC^{TM} comprise no Fourier transformation for deconvolution of the traces, no curve subtraction as the non-reversing response is directly extracted from the isothermal response and no phase lag component to the analysis [10].

Thus, in this work, continuing our studies on the application of polyether-based materials as modern thermal energy storage

* Corresponding author. Tel.: +48 12 6282727; fax: +48 12 6282038.
E-mail address: kpielich@usk.pk.edu.pl (K. Pielichowski).

0040-6031/$ – see front matter © 2005 Elsevier B.V. All rights reserved.
doi:10.1016/j.tca.2005.11.013

systems with increased efficiency [11,12], we present results of the thermal investigations of well-characterised poly(ethylene oxide)/lauric acid blends.

2. Experimental

2.1. Materials

Poly(ethylene oxide) (PEO) was produced by Polysciences Co., Warrington, PA, USA, and its molecular weight was determined by GPC performed at 40 °C on a Hewlett-Packard 1050 GPC System with a refractometric detector, using Shodex OH-Pac SB803 HQ 8 mm × 300 mm column from Showa Denko. DMF was used as the eluent at a flow rate of 0.7 $cm^3\ min^{-1}$, and sample concentration was 1% m/v. GPC data were processed using a GRAMS/386 program (Galactics) to calculate average molecular weights, $M_n = 9630$ and $M_w = 13{,}060$ as well as polydispersity coefficient, $M_w/M_n = 1.38$. ΔH_m was measured as 180.6 J/g and the degree of crystallinity was calculated as 0.92 [13]. A crystalline PEO phase was additionally confirmed by FTIR method (Bio-Rad FTS 165 spectrometer, KBr pellets, resolution 4 cm^{-1}) by the presence of the triplet peak of the COC stretching vibration at 1153, 1106 and 1061 cm^{-1} with a maximum at 1106 cm^{-1} [14].

Lauric acid ($C_{11}H_{23}COOH$) was product of Aldrich Chemical Co. (Steinheim, Germany).

Blends were prepared by mixing weighed amounts of components in the melt, followed by subsequent solidification.

Description of the binary polyether/lauric acid blends is presented in Table 1.

2.2. Techniques

2.2.1. Differential scanning calorimetry

For the DSC measurements a Netzsch DSC 200, operating in dynamic mode, was employed. Samples of ca. 5 mg weight were placed in sealed aluminium pans. The heating/cooling rate of 10 K/min was applied. Argon was used as an inert gas with flow rate 30 $cm^3\ min^{-1}$. Prior to use the calorimeter was calibrated with mercury and indium standards; an empty aluminium pan was used as reference. Liquid nitrogen was used as a cooling medium.

Table 1
Description of the binary polyether/lauric acid blends

Number of sample	Description
1	PEO
2	PEO/lauric acid (9:1, w/w)
3	PEO/lauric acid (8:2, w/w)
4	PEO/lauric acid (7:3, w/w)
5	PEO/lauric acid (6:4, w/w)
6	PEO/lauric acid (5:5, w/w)
7	PEO/lauric acid (4:6, w/w)
8	PEO/lauric acid (3:7, w/w)
9	PEO/lauric acid (2:8, w/w)
10	PEO/lauric acid (1:9, w/w)
11	Lauric acid

2.2.2. Step-scan alternating DSC (SSA–DSC)

Step-scan alternating DSC investigations were performed by using a Perkin-Elmer Pyris Diamond DSC. Measurements were done in closed aluminium pans with sample mass of ca. 8 mg under argon flow of 20 $cm^3\ min^{-1}$. Prior to use the calorimeter was calibrated with indium standard. After a series of optimisation measurements, the following parameters have been chosen: length of the isothermal segment (t_{iso}) = 48 s; linear heating rate in dynamic segments (β) = 2 K/min and temperature jump between two subsequent isothermal segments (step) = 0.25°, 0.5° or 1°.

2.2.3. Infrared spectroscopy (FTIR)

IR spectra of the samples (KBr pellets) were recorded on a Bio-Rad FTS 165 Fourier transform infrared (FTIR) spectrometer at a resolution of 4 cm^{-1}.

2.2.4. Scanning electron microscopy (SEM)

A scanning electron microscope ESEM Philips XL30, equipped with detector of secondary electrons (SE), was used to investigate the surface morphology of carbon-coated samples at the energy of the electron beam of 10 kV.

3. Results and discussion

DSC profiles of the melting and crystallisation of samples 1–11 are presented in Figs. 1 and 2.

Results of DSC investigations for PEO and PEO/lauric acid blends show that the temperature range and heat of phase transition depend on the composition of the blends—with an increase of PEO content, a shift of the maximum of melting peak of PEO towards higher temperatures and of lauric acid to lower temperatures can be observed.

The presence of two different substances in blends causes that their crystallisation is hindered and depends on the ratio of components. From the course of DSC profiles of blends

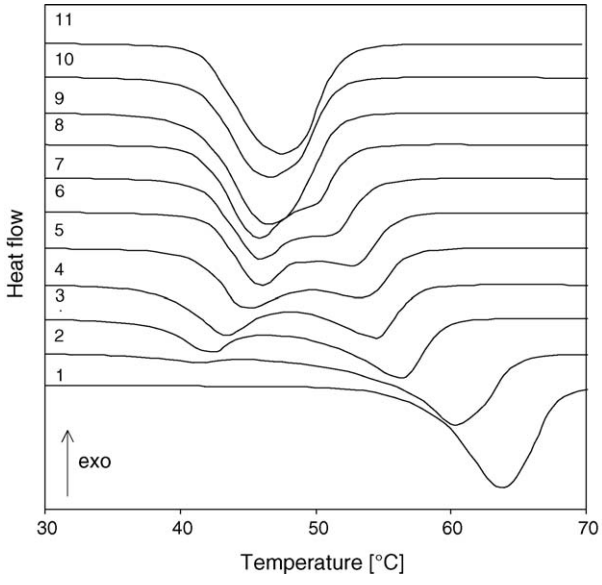

Fig. 1. DSC profiles of the melting process of samples 1–11.

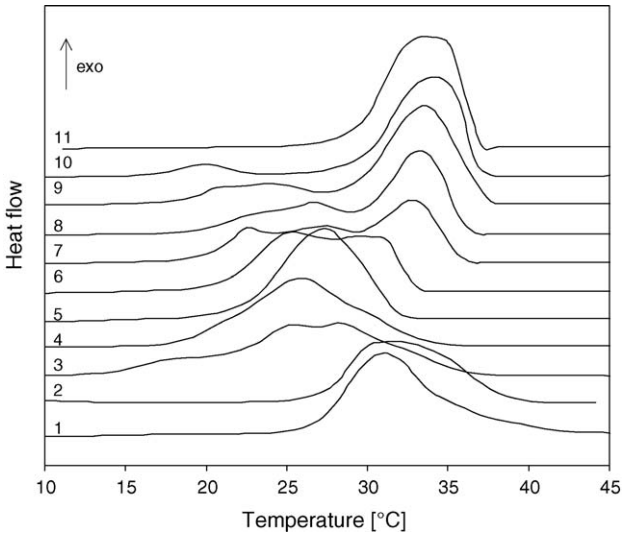

Fig. 2. DSC profiles of the crystallisation process of samples 1–11.

crystallisation process it could be seen that peaks originating from exothermic crystallisation processes of PEO and lauric acid overlaps and only for PEO/lauric acid (1:9, w/w) blend the crystallisation peaks are clearly separated.

For blends of PEO/lauric acid (9:1, 8:2, 7:3 and 6:4, w/w) one crystallisation peak has been detected while during melting two peaks occurred.

Generally, crystallisation process of polymers is more difficult and there is a larger supercooling effect than for low-molecular-weight compounds. Accordingly, the degree of supercooling for lauric acid is considerably lower than for PEO and in spite of differences in melting temperatures of both substances they crystallise in the blend in the same temperature range.

For other blends two maxima on DSC curves have been observed—with an increased content of lauric acid, crystallisation process of PEO is more and more hindered and more defected structures are formed that are characterised by lower melting temperatures. They cause a higher supercooling effect and thus a shift of solidification peaks to the lower temperatures.

It can be also observed that melting process covers the widest temperature range in case of PEO 10,000/lauric acid (9:1, w/w) blend. Analysis of the DSC data revealed that the highest value of enthalpy of phase transition characterises the (1:1, w/w) PEO/lauric acid blend (Tables 2 and 3).

To compare the difference between experimental and theoretical values of the heats of phase transition theoretical values have been calculated, according to the relationship

$$\Delta H_b = \Delta H_p x_p + \Delta H_a x_a$$

where ΔH_b is the heat of phase transition of the blend, ΔH_p the heat of phase transition of the polymer, ΔH_a the heat of phase transition of the acid, and x_p and x_a are the weight fractions of polymer and acid, respectively.

Results are presented in Fig. 3.

It can be observed that for PEO blends experimental values are higher that expected from theoretical calculations. This effect

Table 2
Thermal parameters and heat of melting of samples 1–11

Sample	T_{onset} (°C)	T_{end} (°C)	T_{max} (°C)	Heat of melting (J/g)
1	57.8	67.9	63.7	177.8
2	36.0	63.7	41.4 60.4	183.2
3	37.9	59.6	42.3 56.2	177.1
4	38.8	57.5	43.4 54.4	184.9
5	41.3	56.9	45.0 53.3	182.5
6	42.1	55.8	45.9 52.5	208.3
7	41.6	54.3	46.0 50.1	180.0
8	41.5	52.7	45.8 49.3	177.2
9	41.2	51.6	46.7	194.7
10	41.4	51.5	46.6	181.0
11	41.6	51.8	47.5	183.8

is due to the facilitated formation of hydrogen bonding between the hydrogen atoms from the carboxylic acids groups in lauric acid and the ether oxygen from the polyoxyethylene chains. Indeed, the FTIR spectrum of the PEO/lauric acid blend, dis-

Table 3
Thermal parameters and heat of crystallisation of samples 1–11

Sample	T_{onset} (°C)	T_{end} (°C)	T_{max} (°C)	Heat of crystallisation (J/g)
1	36.1	26.6	31.1	170.0
2	37.7	25.9	33.0 8.1	178.9
3	35.9	14.0	28.3 25.3 18.8	169.0
4	33.6	18.3	25.9	174.8
5	34.9	22.5	27.4	178.3
6	32.9	21.0	30.6 29.2 25.3	202.0
7	35.7	20.0	32.8 27.3 22.3	175.0
8	36.1	19.4	33.1 26.6	173.9
9	37.4	18.4	33.6 23.8 21.2	194.9
10	36.9	16.6	34.2 20.0	171.0
11	36.4	29.4	33.6	184.8

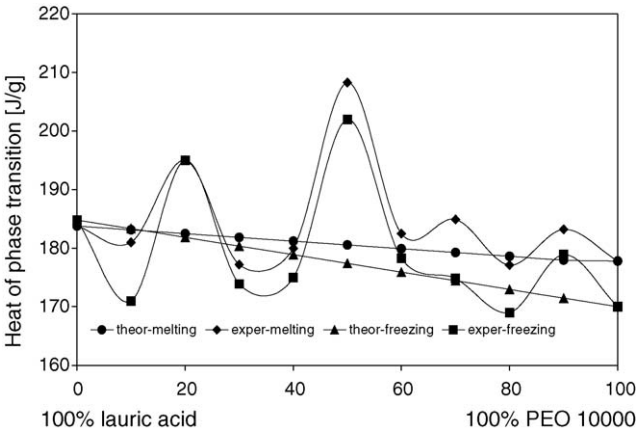

Fig. 3. Comparison of the theoretical and experimental values of the heats of phase transition of PEO/lauric acid blends.

played in Fig. 4, shows a shift of 30 cm^{-1} of the –OH absorption band in the 3400–3550 cm^{-1} range.

Analysis of the FTIR spectrum of the lauric acid indicates also that the carboxylic acid forms a dimeric structure (C=O stretching band at 1705 cm^{-1}), and there is no esterification reaction between PEO and the acid, as evidenced by PEO/lauric acid spectrum.

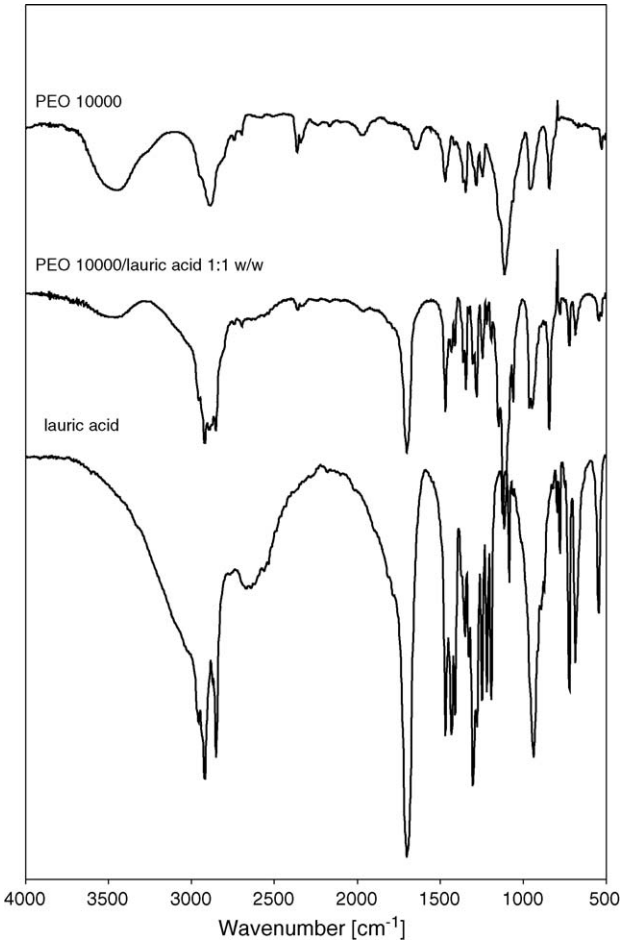

Fig. 4. FTIR spectra of samples PEO, lauric acid and PEO/lauric acid (1:1, w/w) blend.

The existence of hydrogen bonding enhances formation of lamellar texture, as it is shown in Fig. 5.

Morphology arrangement of the PEO/lauric acid blends is basically similar to the morphology of pure lauric acid. Generally, carboxylic acids crystallise in orthorhombic or monoclinic systems, retaining dimer forms, as it was confirmed by FTIR analysis, and forming parallelly arranged crystals that can be seen in Fig. 5 for lauric acid. In the blend there are no spherulitic structures that are typical for PEO—it could be assumed that the presence of an acid in blend causes hindered crystallisation of PEO and leads to a decrease of PEO crystallinity and formation of larger amounts of metastable or amorphous regions. In consequence, blends' texture resembles crystal arrangement of pure lauric acid.

One can also observe that metastable amorphous regions are present between the crystallites that origin form PEO and lauric acid. One can also consider formation of a kind of association complex where an ordering of acid molecules along the poly(ethylene oxide) chain occurs; in the presence of polymer the unfavourable entropic contribution is reduced to the extent that enthalpic factor prevails and complexation is possible—this assumption needs however a more detailed investigation. In the liquid state poly(ethylene oxide) and lauric acid are miscible over the whole concentration range—after mixing of the blend's components homogeneous, clear liquids are obtained.

Phase separation which occurs in the blend in the solid state is a result of differences in the temperatures of melting and solidification and supercooling between poly(ethylene oxide) and lauric acid (polymers are generally characterised by higher supercooling than low-molecular-weight compounds). During cooling of PEO/lauric acid blends, in the first stage crystallises lauric acid and then PEO (as shown previously in Fig. 2). As a result, PEO crystallises under high viscosity conditions of the alloy and at relatively low temperatures in limited free volumes between lauric acid crystals, leading eventually to the phase separation of the blends in solid state.

MT-DSC is a relatively new technique that offers extended temperature profile capabilities by, e.g., sinusoidal wave superimposed to the normal linear temperature ramp

$$T = T_0 + \beta t + B\sin(\omega t) \quad (1)$$

where T is the program temperature, T_0 the starting temperature, β the underlying average heating rate, B the amplitude of the temperature modulation and $\omega = 2\pi/p$ (s^{-1}), is the modulation angular frequency.

The superimposition may be also in form of oscillations, dynamic-isothermal heating and cooling segments, "saw-tooth" profile, etc.

The equation to describe heat flow is derived from a simple equation based on thermodynamic theory in which

$$\frac{dQ}{dt} = C_{pt}\frac{dT}{dt} + f(t, T) \quad (2)$$

where Q is the amount of heat absorbed by the sample, C_{pt} the thermodynamic heat capacity and $f(t, T)$ is some function of time and temperature that governs the kinetic response of any physical or chemical transformation [15].

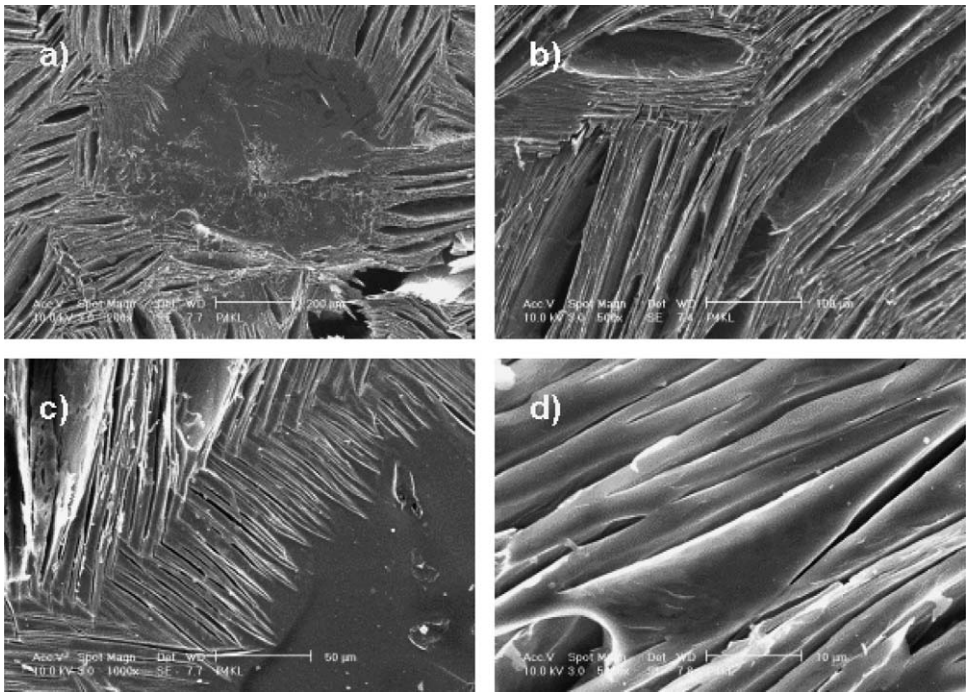

Fig. 5. SEM microphotographs of PEO/lauric acid (1:1, w/w) blend. Magnification: (a) 200×, (b) 500×, (c) 1000× and (d) 5000×.

By assuming that the temperature modulation is small and that over the interval of the modulation the response of the rate of the kinetic process to temperature can be approximated as linear, one can rewrite Eq. (2) as

$$\frac{\mathrm{d}Q}{\mathrm{d}t} = C_{\mathrm{pt}}(\beta + B\omega\cos(\omega t)) + f'(t, T) + C\sin(\omega t) \tag{3}$$

where $f'(t, T)$ is the average underlying kinetic function once the effect of the sine wave modulation has been subtracted, C the amplitude of the kinetic response to the sine wave modulation and $(\beta + B\omega\cos(\omega t))$ is the measured quantity $\mathrm{d}T/\mathrm{d}t$.

The kinetic approach is based on differentiating between fast responses (equilibrium behaviour) and slower kinetically hindered processes including irreversible processes.

Eq. (3) can be rewritten as

$$\Phi(T(t)) = \Phi_{\mathrm{dc}}(T(t)) + \Phi_{\mathrm{a}}(T(t))\cos(\omega_0 t - \varphi) \tag{4}$$

where Φ is the phase shift, Φ_{a} the cyclic component and Φ_{dc} is the underlying heat flow.

We obtain the reversing component of the heat flow from

$$\Phi_{\mathrm{rev}}(T(t)) = \frac{\Phi_{\mathrm{a}}(T(t))}{B\omega_0}\beta_0 \tag{5}$$

The kinetic component (the non-reversing component) is then

$$\Phi_{\mathrm{non}}(T(t)) = \Phi_{\mathrm{dc}}(T(t)) - \Phi_{\mathrm{rev}}(T(t)) \tag{6}$$

The modulated temperature and resultant modulated heat flow can be deconvoluted using a Fourier transform to give reversing and non-reversing components. The reversing component is evaluated from the periodic part of the heat flow. The non-reversing component is the difference between the underlying heat flow (static heat flow) and the reversing component. The static heat flow is evaluated by an averaging method. Amplitude of the cyclic response and the phase lag are divided into in and out of phase responses by use of the phase lag unless the phase shift is small in which case the out of phase component can be neglected [16].

An alternative evaluation method has been reported based on the linear response approach [17]. In this method, the heat flow rate into the sample is described as

$$\Phi(t) = \int_0^t \dot{C}(t - t')\beta(t')\,\mathrm{d}t' \tag{7}$$

with

$$\beta(t) = \beta + \omega_0 B\cos(\omega_0 t) \tag{8}$$

Insertion of Eq. (8) into Eq. (7) leads to the relationship

$$\Phi(T(t)) = C_\beta(T)\beta + \omega B|C(T, \omega)|\cos(\omega t - \varphi) \tag{9}$$

with

$$|C| = \sqrt{C'^2 + C''^2} \tag{10}$$

where C' is the storage heat capacity (associated with mobility) and C'' is the loss heat capacity (associated with dissipation).

Both the phase shift and the amplitude of the dynamic component are used for the calculation of a complex (frequency-dependent) heat capacity. These quantities can be interpreted in the context of the relaxation theory or irreversible thermodynamics.

In the step-scan alternating DSC, the temperature program comprises a periodic succession of short, linear heating and isothermal phases; the measured heat flow contain thus fractions which arise from the heat capacity and those due to physical transformations or chemical reactions [18].

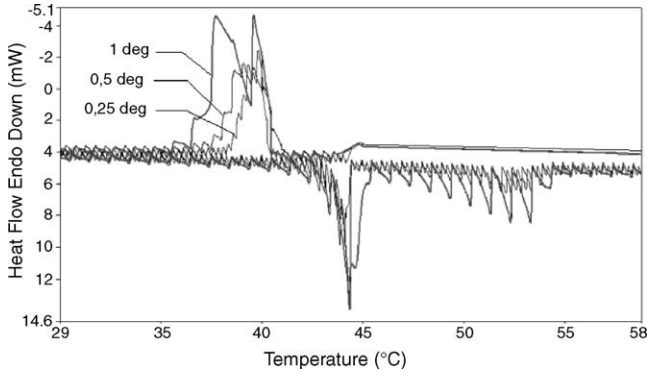

Fig. 6. SSA–DSC curves of PEO/lauric acid (1:1, w/w) blend with different steps.

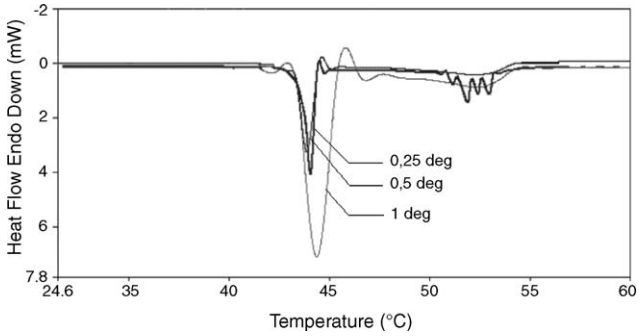

Fig. 8. SSA–DSC non-reversing component of the melting process of PEO/lauric acid (1:1, w/w) blend with different steps.

Since there is no complex Fourier transform involved in data deconvolution and no phase lag component to the analysis, the reported advantages include reliable and direct heat capacity measurement with low mass samples over a much shorter time than experiments performed in equivalent large mass heat flux modulated temperature DSC.

More information about the nature of thermal transitions in polymeric materials can be gained if modulated temperature differential scanning calorimetry (MT-DSC) is applied. SSA–DSC profiles of the PEO/lauric acid (1:1, w/w) blend, which showed the highest values of the heats of phase transition, are presented in Fig. 6.

It can be observed that an increase of the temperature step causes that the average total heating rate is also increasing and the heat flow is characterised by higher values.

The reversing component of the heat flow during melting (Fig. 7) reaches its lowest values at the highest step (step = 1°) when the re-crystallisation of PEO is hindered.

MT-DSC has proved to be useful method for studying the dynamic processes taking place at the growing crystal faces. Wunderlich and Okazaki employed a quasi-isothermal mode of MT-DSC in a study on PET, in which from the intensity of the periodic signal the fraction of crystallites undergoing at a given temperature a reversible local melting could be deduced [19]. Similar study was also performed for PEEK [20]. Temperature coefficient of the growth rate of the PE and PET crystallites was found to be phase lag- and heat flow-dependent [21,22]. Syndiotactic PP (which has a well-defined morphology, being composed of stacks of laterally extended lath-shaped crystallites with a uniform thickness of 5–10 nm, whereby the amorphous layers between the lamellae show a broad distribution with an average thickness of ca. 15 nm) melts from its local surfaces only and the kinetic shows up in the imaginary part of the complex specific heat. Observations are indicative for the occurrence of reversible local melting-crystallisation processes at the crystal surfaces, which may well take place in the melt close to the crystal face [23]. Experimental results confirmed that C'' increases linearly with the underlying mean heating rate and the modulation period; besides, C'' was inversely related to the superheating (related to the volume of the crystallites) effective during melting [24].

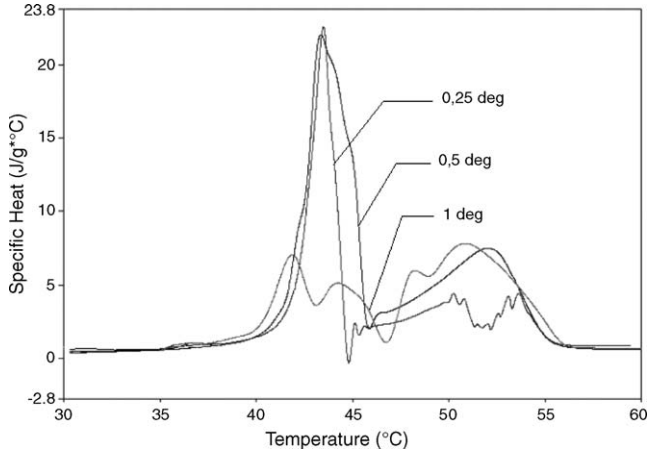

Fig. 7. SSA–DSC reversing component of the melting process of PEO/lauric acid (1:1, w/w) blend with different steps.

In the non-reversing signal of the melting process peak of the lauric acid dominates and the calorimetric signal of the PEO melting is rather small (Fig. 8).

Based on the "classical" DSC results, which revealed that heats of melting of lauric acid and PEO (average molecular weight 10,000) are similar (187.7 and 180.6 J/g, respectively), one can assume that crystallisation of PEO is less intensive that organisation process of lauric acid. One can consider formation of a kind of association complex where an ordering of acid molecules along the poly(ethylene oxide) chain occurs; in the presence of polymer the unfavourable entropic contribution is reduced to the extent that enthalpic factor prevails and complexation is possible.

Analysis of the crystallisation process is related mainly to the non-reversing component since reversing signal is usually perturbed (Fig. 9).

Schawe and Bergmann [25] investigated the melting of poly(ethylene terephthalate) (PET) and poly(ε-caprolactone) (PCL) by MT-DSC and proposed four models to describe the complex phase behaviour of polymers that contain non-equilibrium crystals as well as amorphous material resulting in local processes close to the surface. The models describe different melting regimes that are: (i) running very fast, (ii) running

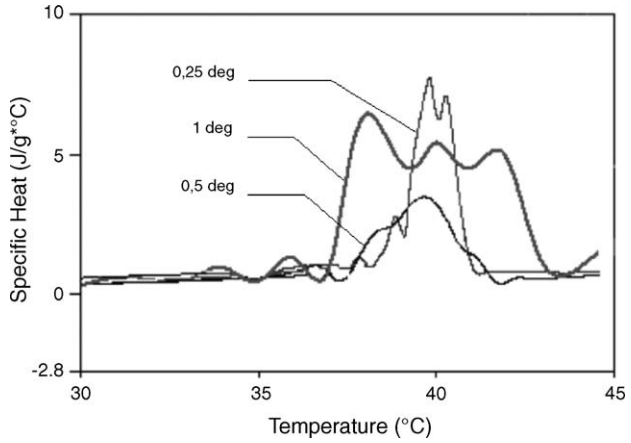

Fig. 9. SSA–DSC reversing component of the crystallisation process of PEO/lauric acid (1:1, w/w) blend with different steps.

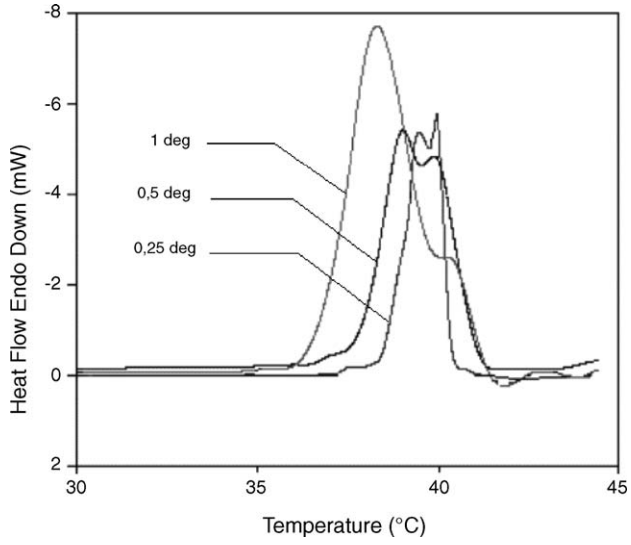

Fig. 10. SSA–DSC non-reversing component of the crystallisation process of PEO/lauric acid (1:1, w/w) blend with different steps.

with a constant melting rate, (iii) like (ii) + relaxation process and (iv) like (i) + kinetic process. It has been found that model (iv) yielded best approximation for the simultaneously melting of different types of crystals that are usually present in semi-crystalline polymers.

As it can be seen in Fig. 10, crystallisation peaks of lauric acid and PEO are overlapped due to supercooling effect of macromolecular compound. By smaller steps this effect also becomes smaller and there is a change in mutual proportions.

An increase of step generally leads to an increase of the number of non-equilibrium effects and facilitates the activation of kinetic non-reversing processes, hindering the overall crystallisation of PEO. For lauric acid, due to facile crystallisation and self-association, formation of ordered regular structures takes place faster and is influenced by non-reversing processes in higher proportion.

4. Conclusions

Poly(ethylene oxide)/lauric acid blends show high values of heat of melting and crystallisation which exceed theoretically determined values; the PEO/lauric acid blend (1:1, w/w) blend was characterised as displaying the highest values of heat of transition, determined by DSC method. Further studies by SSA–DSC revealed that an increase of the temperature step causes that the average total heating rate is also increasing and the heat flow is characterised by higher values. The reversing component of the heat flow during melting reaches its lowest values at the highest step (step = 1°) when the re-crystallisation of PEO is hindered. Since in the non-reversing signal of the melting process peak of the lauric acid dominates and the calorimetric signal of the PEO melting is rather small, one can consider formation of a kind of association complex where an ordering of acid molecules along the poly(ethylene oxide) chain occurs; in the presence of polymer the unfavourable entropic contribution is reduced to the extent that enthalpic factor prevails and complexation is possible.

Acknowledgement

The authors are grateful to the Polish Committee for Scientific Research (Grant No. PB 0975/T09/2002/22) for financial support.

References

[1] M.W. Babich, R. Benrashid, R.D. Mounts, Thermochim. Acta 243 (1994) 193.
[2] M.W. Babich, S. Hwang, R.D. Mounts, Thermochim. Acta 226 (1993) 163.
[3] K. Pielichowski, Eur. Polym. J. 35 (1999) 27.
[4] S.M. Hasnain, Energy Convers. Manage. 39 (1998) 1127.
[5] D. Feldman, D. Banu, Thermochim. Acta 272 (1996) 243.
[6] K. Pielichowski, K. Flejtuch, Polym. Adv. Technol. 13 (2002) 690.
[7] S.Z.D. Cheng, J.S. Barley, P.A. Giusti, Polymer 31 (1990) 845.
[8] F.E. Bailey, J.V. Koleske, Poly(ethylene oxide), Academic Press, New York, 1976.
[9] A. Sari, K. Kaygusuz, Solar Energy 71 (2001) 356.
[10] http://www.perkinelmer.com.
[11] K. Pielichowski, K. Flejtuch, Macromol. Mater. Eng. 288 (2003) 259.
[12] K. Pielichowski, K. Flejtuch, J. Appl. Polym. Sci. 90 (2003) 861.
[13] http://web.utk/athas.
[14] X. Li, S.L. Hsu, J. Polym. Sci. Polym. Phys. 22 (1984) 1331.
[15] M. Reading, A. Luget, R. Wilson, Thermochim. Acta 238 (1994) 295.
[16] M. Reading, Trends Polym. Sci. 248 (1993) 1.
[17] J.E.K. Schawe, Thermochim. Acta 260 (1995) 1.
[18] M. Sandor, N.A. Bailey, E. Mathiowitz, Polymer 43 (2002) 279.
[19] I. Okazaki, B. Wunderlich, Macromolecules 30 (1997) 1758.
[20] A. Wurm, M. Merzlyakov, C. Schick, Colloid Polym. Sci. 276 (1998) 289.
[21] A. Toda, T. Oda, M. Hikosaka, Y. Surayama, Polymer 38 (1997) 231.
[22] A. Toda, C. Tomota, M. Hikosaka, Y. Surayama, Polymer 38 (1997) 2849.
[23] J. Schmidtke, G. Strobl, T. Thurn-Albrecht, Macromolecules 30 (1997) 5804.
[24] J.E.K. Schawe, G.R. Strobl, Polymer 39 (1998) 3745.
[25] J.E.K. Schawe, E. Bergmann, Thermochim. Acta 304/305 (1997) 179.